



Review Paper

Study of the influence of friction stir processing on tungsten inert gas welding of different aluminum alloy

Husain Mehdi¹  · R. S. Mishra¹

© Springer Nature Switzerland AG 2019

Abstract

Tungsten inert gas welding is the most commonly used process for joining of aluminum alloy, which are highly demanded in aerospace application. In this process coarse grain structure, micro crack and porosity was obtained due to persisting thermal conditions when the fusion zone start to solidify. The formation of these defects on the weld region will result in reduction of weld strength about to half the parent material. To avoid these defects the top surface of gas tungsten arc welding are processed using friction stir processing up to certain depth from the top of the welds. Friction stir processing destroyed the coarse grain dendritic structure in the tungsten welded joint, because of change in grains refinement and microstructure significantly improved the hardness of the friction stir processing (FSP) weld over the base metal and TIG weld. In this study, we compared the experimental result of TIG, FSW and (TIG + FSP) welded joint. Coarse grain structure was observed in TIG welding and fine grain structure was observed in FSP process. In addition very fine grain structure we observed in stir zone due to the effect of intense plastic deformation and temperature during TIG + FSP.

Keywords Tensile strength · Microstructure analysis · Micro-hardness · Friction stir welding

1 Introduction

Friction stir welding (FSW) is a new technique of joint similar and dissimilar materials and it is environmental friendly and energy efficient [1, 2]. The friction stir welding has been successfully used to produce joint in Mg-alloy, Al-alloy, Ti-Alloy and other alloy [3–7]. Comparison between TIG and FSW technique with a long established one the friction stir welding shown the advantages to tungsten inert welding. The used material Al-6082-T6 makes high claims to these techniques due to the problem of pore formation and hot cracks [8]. Another problem is the loss of strength and hardness caused by the microstructural instability in the heat affected zone (HAZ) [9].

In the recent year, FSW has been a research focus instead of TIG welding. Comparison to other welding process, FSW is versatile for magnesium alloy, aluminum alloy, copper alloy, steel and dissimilar alloy [10–15]. It is widely used for Al–Zn and Al–Cu series which have a poor

performance [16–21]. The carbon migration takes place in dissimilar welded joint subjected to thermal loading at temperature of 625°. The micro-hardness and ultimate tensile strength of welded joint increase by increasing the pre-stress [22–24].

There are several techniques applied such as heat treatment process, gas tungsten arc welding (TIG), arc melting and mechanical deformation process to modify the material properties in order to improve the joint properties. However these methods are not efficient and some of those are not applicable for using welded joints, where the joint strength is highly required. In recent year, friction stir welding becomes a prominent welding process for joining of aluminum alloy [1]. The joining of aluminum alloy magnesium alloy can be easily weld by FSW process, moreover, it is also suitable for joining of dissimilar material [25–31]. Friction stir welding involves a cylindrical rotating tool of consumable or non-consumable material that plunges between the two plates and moves, stir and bounded

✉ Husain Mehdi, husainmehdi4u@gmail.com | ¹Department of Mechanical Engineering, Delhi Technological University, New Delhi, India.



between them. The heat is produced during FSW process and generation of thermo-mechanical conditions develops a heterogeneous fine grained microstructure across the weld seam [32]. The stirred zone materials to soften without melting of parent material due to heat generated by the process of adiabatic heat and mechanical mixing with in the material [33]. The mechanical properties of FSW joint are mainly dependent on chemical composition and processing parameters of alloying element. The microstructural analysis of FSW joints shows the formation of new grain size in the weld zone with different amount of heat input by controlling the processing parameter [34–37].

The coarse grain structure, micro-cracks and porosity are obtained in TIG welding due to the unremitting thermal conditions. Forming these defects on the weld zone will result in a reduction in weld strength. In this work, to avoid these defects, a friction stir processing is used to destroy the coarse-grained dendritic structure in the tungsten welded joint and very fine grain structure was observed in stir zone to the effect of intense plastic deformation and temperature during TIG + FSP.

2 Materials and method

2.1 Selection parameter for TIG welding

When TIG welding is applied, rust, paint, dirt oil and other contamination must be removed from the welded material surface. The welding properties is also depended on the electrode condition, arc length, travel speed, current polarity on weld shape, shielding gas coverage and angle of the torch. The welding parameter ranges taken into account for welding arc welding current of 120–180 amp gas flow rate of 15 L/min and welding speed of 90–105 mm/min.

2.2 Selection parameter for FSW

After TIG welding on aluminum alloy, friction stir welding was applied on TIG welded joint. FSW involve plastic

deformation and complex movement. FSW processing parameter such as welding speed, tool rotation and axial force on the welding characteristics. Weld were made by joining of two plates (200 × 60 × 7 mm) workpiece were clamped on the machine tool.

2.3 Experimental procedure

The aluminum alloy used in this study in the form of plates with the dimension of (200 × 60 × 7 mm). The plates were cleaned with the help of acetone to remove the oil the oil and dirt etc. and steel wire brush was used to remove the oxide layer. During TIG welding. The optimized welding parameter such as welding current of 120 amp, a voltage of 20 V and the welding speed of 34 mm/min and argon shielding are used. Before friction stir welding the GTAW weld reinforcement are removed by machining it and flattened the weld bead with its substrate sides for applying better friction stir processing, after marching of GTAW weld, FSP was applying at the transverse speed of 1.1 mm/sec, target depth of 2 mm, rotational speed of 1200 rpm and vertical force of 8000 kg applied over the weld during FSP. The cylindrical tool was used during FSP of EN31 with pin length of 2 mm. The pin and shoulder diameter of FSP tool were 6 mm and 18 mm respectively [39].

3 Results and discussions

3.1 Tensile strength

The ultimate tensile strength of welded joint of Al-6083-T6 and Al-2024 has been investigated by using of TIG, FSW and (TIG + FSP) welding process at different process parameter as shown in Fig. 1. The average tensile strength and their corresponding percentage elongation as shown in Tables 1 and 2 for TIG and FSW respectively. In each condition three specimen were tested. The chemical composition for Al-6083-T651 and Al-2024 as shown in Tables 3 and 4. The minimum ultimate tensile strength of 204.23 MPa was obtained at 160 amp current in TIG welding, whereas

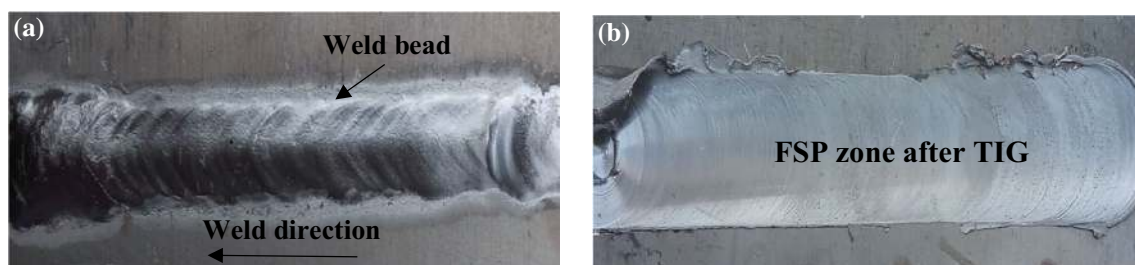


Fig. 1 Weld bead formation and quality of weld, **a** TIG welding, **b** TIG + FSP

Table 1 Processing parameter of TIG welding [38]

Specimen designation	Current (amp)	Gas flow rate (l/min)	Tensile strength (MPa)	Microhardness (HV)	Percentage elongation	Impact toughness
B ₁	120	15	165	49	3.53	6
B ₂	140	15	204	57	4.52	8
B ₃	160	15	186	54	4.21	5
B ₄	180	15	173	49	4.11	4

Table 2 Processing parameter of friction stir welding [38]

Exp. no.	Tool speed (rpm)	Welding speed (mm/min)	Axial force (KN)	Tensile strength (MPa)	Percentage elongation	Micro-hardness (HV)	Impact toughness
1	300	25	6	202	5.4	52	15
2	700	25	6	221	6.4	55	19
3	500	15	6	229	6.3	58	15
4	500	35	6	244	7.8	60	18
5	500	25	4	234	5.8	57	16
6	500	25	8	250	6.7	55	20
7	500	25	6	265	7.1	65	24

Table 3 Chemical composition of Al-6082-T651 [38]

Si	Cu	Fe	Mg	Mn	Zn	Cr	Ti	Al
0.7–1.3	0.1	0.5	0.6–1.2	0.4–1.0	0.2	0.25	0.2	Balance

Table 4 Chemical composition of Al-2024 [39]

Si	Cu	Fe	Mg	Mn	Zn	Cr	Ti	Al
0.5	3.9	0.48	1.45	0.58	0.24	0.09	0.148	Balance

maximum ultimate tensile strength of 223.65 MPa at tool rotation of 500 rpm, welding speed of 25 mm/min and axial force of 6KN was obtained in FSW process. The strength of both at GTAW and GTAW + FSP welds are lower than the parent material as shown in Figs. 2 and 3. The strength of TIG weld and TIG + FSP, however TIG + FSP joint showed better performance and its elongation is higher than the TIG welds. The ductility of the TIG + FSP welds are better than the TIG welds due to absence of porosity and other defects and improved microstructure characteristics.

3.2 Micro-hardness

In this study, 2 mm thick cold rolled annealed and 6 mm thick hot rolled plate Al–Mg–Mn–Sc–Zr alloy were examined to study the effect of FSW and tungsten inert gas welding process on the microstructure and mechanical properties of welded joints as shown in Table 5.

Figure 4 shows the micro-hardness of FSW and TIG welded joint for cold rolled annealed and hot rolled

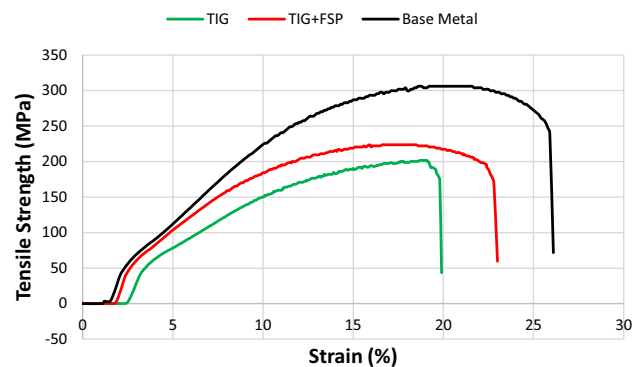


Fig. 2 Comparison of stress strain diagram of Al-2024 for base metal, TIG and TIG + FSP

aluminum alloy plate. The micro-hardness value for both the welding processes are low at the center of welded joint and the microhardness of the welded joint higher than the base material [43]. For hot rolled and cold rolled plate,

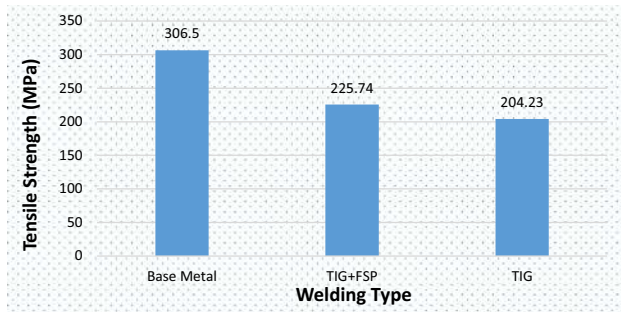


Fig. 3 Comparison of tensile strength of Al-2024 for two different welding process TIG and TIG + FSP

Table 5 Tensile mechanical properties of base metal and welded joints [43]

Sample	Tensile strength (MPa)	Yield strength (MPa)	Elongation (%)
Hot rolled plate			
Base plate	411	290	19.6
FSW joint	380	239	12.5
TIG joint	344	227	9.5
Cold rolled plate			
Base plate	423	322	20.7
FSW joint	391	257	10.9
TIG joint	365	246	10.2

the micro-hardness at FSW center is higher than the TIG weld center and the yield point stress of aluminum alloy is directly proportional to its hardness [46]. The distribution of micro-hardness is consistent with the result that tensile test sample of friction stir welding all broke at the weld center (Table 6).

The hardness values of the TIG welds HAZ region exhibit higher hardness over the HAZ of the TIG + FSP joint. The distance away from the weld center towards unaffected

Table 6 Mechanical properties of Al-6082-T651 [38]

Ultimate tensile strength (MPa)	Yield strength (MPa)	Percentage elongation	Hardness (HV)
312–322	260	10–13	94

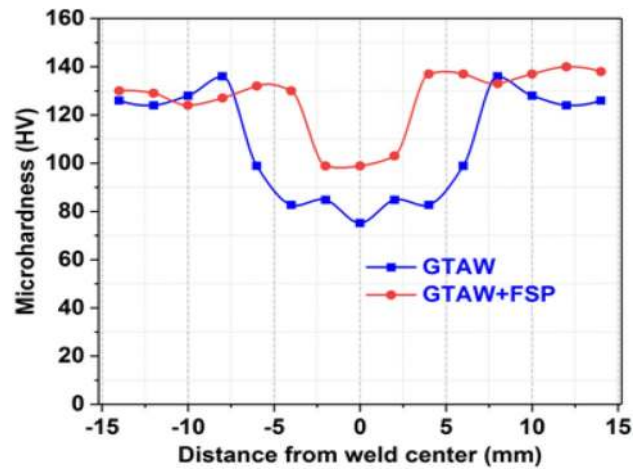


Fig. 5 Microhardness of welded joint at two different welding processes TIG and TIG + FSP [39]

base metal, the HAZ region after the TMAZ, in this zone the joints temperature is comparatively low and at this low temperatures, this zone experienced to induce a kind of ageing, hence it's resulted in an enhancement of mechanical properties. As a matter of fact, the microhardness of TIG + FSP joints as shown in Fig. 5 clearly indicates the lowest hardness value are related to the TMAZ region and stir zone, while the hardness of HAZ region are slightly higher compared to the even un affected base metal. As seen from the microstructures and modified microstructure of the TIG + FSP weld of fine grain structure over the TIG coarse grain structure, the hardness distribution directly indicates the evidence of improved microstructural characteristics and mechanical properties of the TIG + FSP weld [39].

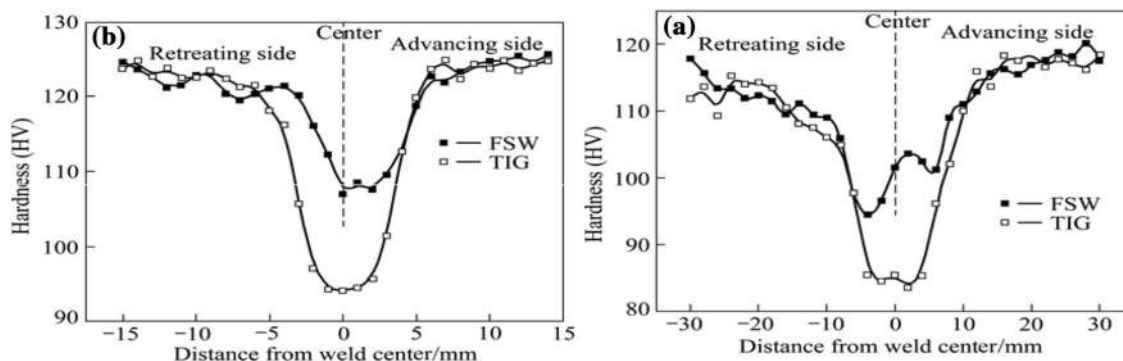
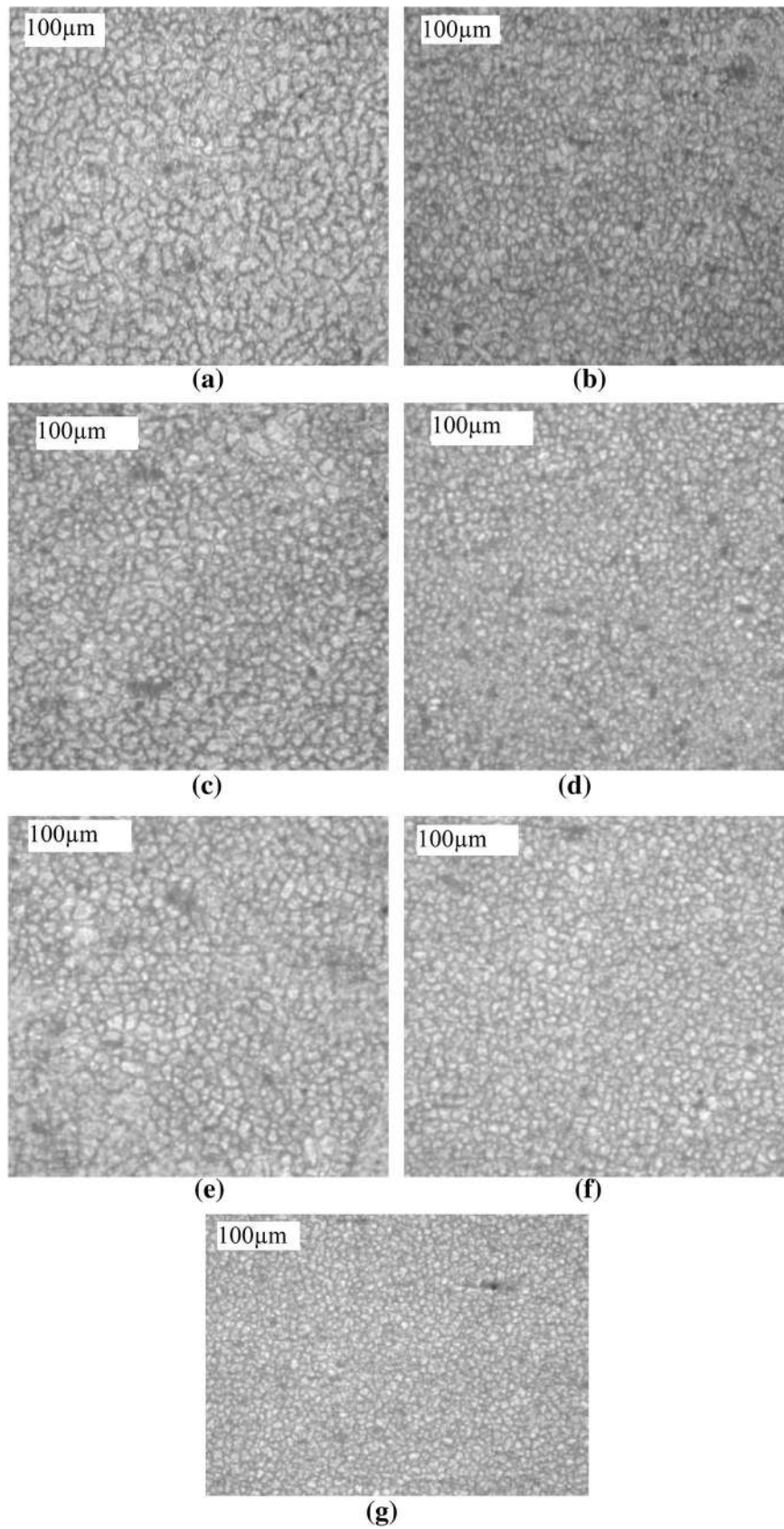


Fig. 4 Microhardness of the welded joint, **a** cold rolled annealed plate, **b** hot rolled plate [43]

Fig. 6 Optical micrograph of FSW for Al-alloy specimen from the experiment No 1 to 7 (at $\times 100$) [38]



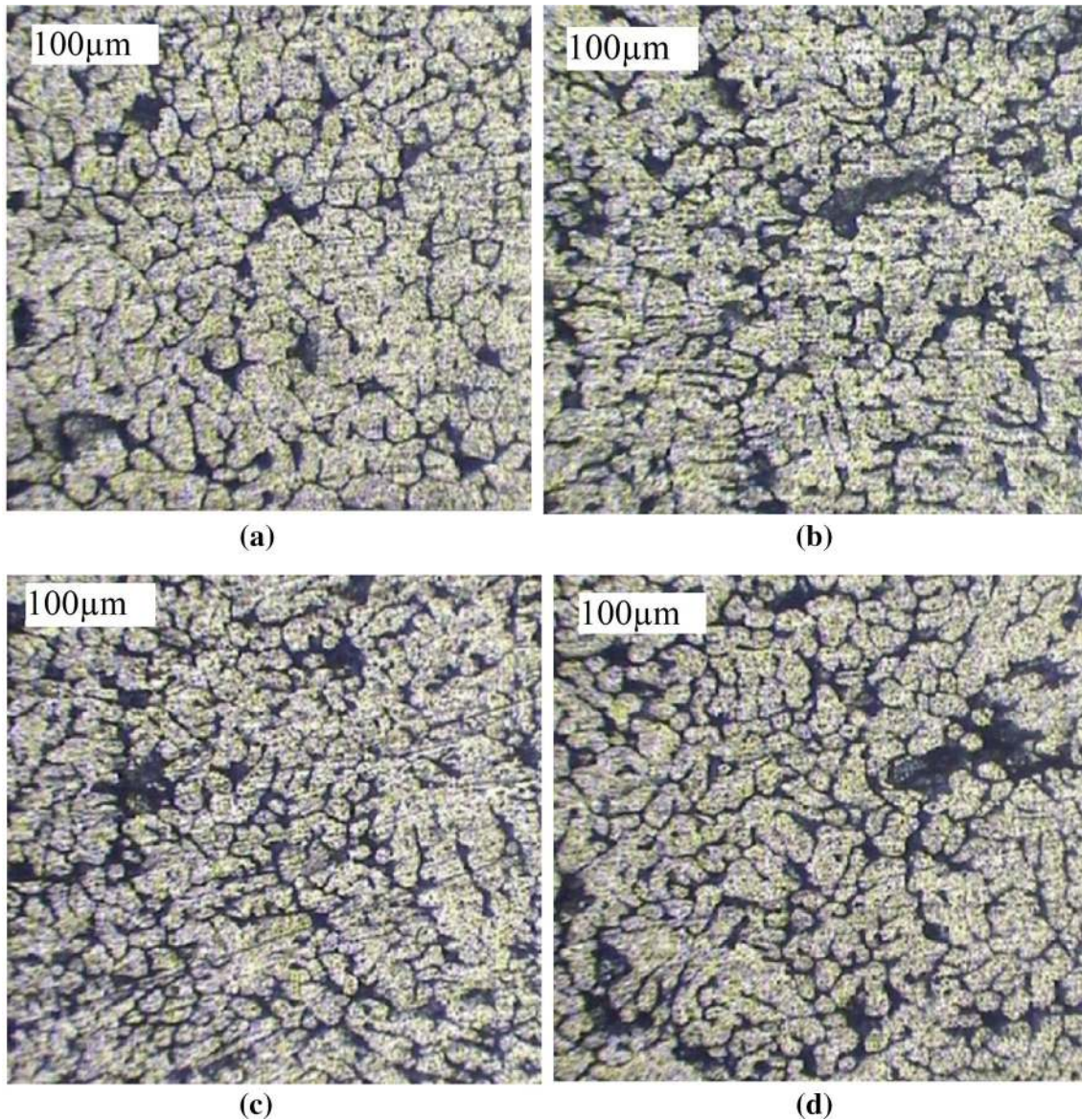


Fig. 7 Optical micrograph of TIG welded joint at different current, **a** 120 amp, **b** 140 amp, **c** 160 amp, **d** 180 amp

3.3 Microstructure analysis of TIG, FSW and (TIG + FSP)

3.3.1 Optical micrograph of FSW and TIG welded joints

Figures 6 and 7 illustrate the optical micrograph of FSW and TIG welded joints. The microstructure of the FSW joint, the weld region of FSW contain equiaxed and finer grain structure and TIG welded shows the elongated and coarse grain structure. The distribution of precipitates were different in TIG and FSW welded joint [40–42]. Due to equiaxed and finer grain structure in FSW and dendrite structure in TIG welded joint and the tensile strength of FSW joint was higher than the TIG welded joint.

During the welding process, the temperature at TIG weld center was higher than the FSW weld nugget zone, and the temperature at TIG weld center was higher than melting point of the alloy. Figure 8a–d, shows the optical microstructure of TIG welded joint. It shows the weld center of cold rolled annealed and hot rolled plate exhibits cast structure and the grain size of TIG welded joint of hot rolled plate, there are a few short feathery or pine tree structure (Fig. 8a), the boundary of semi-molten zone and heat affected zone (HAZ) is obvious (Fig. 8b), and there is very thin layer of equiaxed grains between the semi fused zone and the heat affected zone, the equiaxed and smaller than the grain structure of fused zone and HAZ as shown in Fig. (8c) [43].

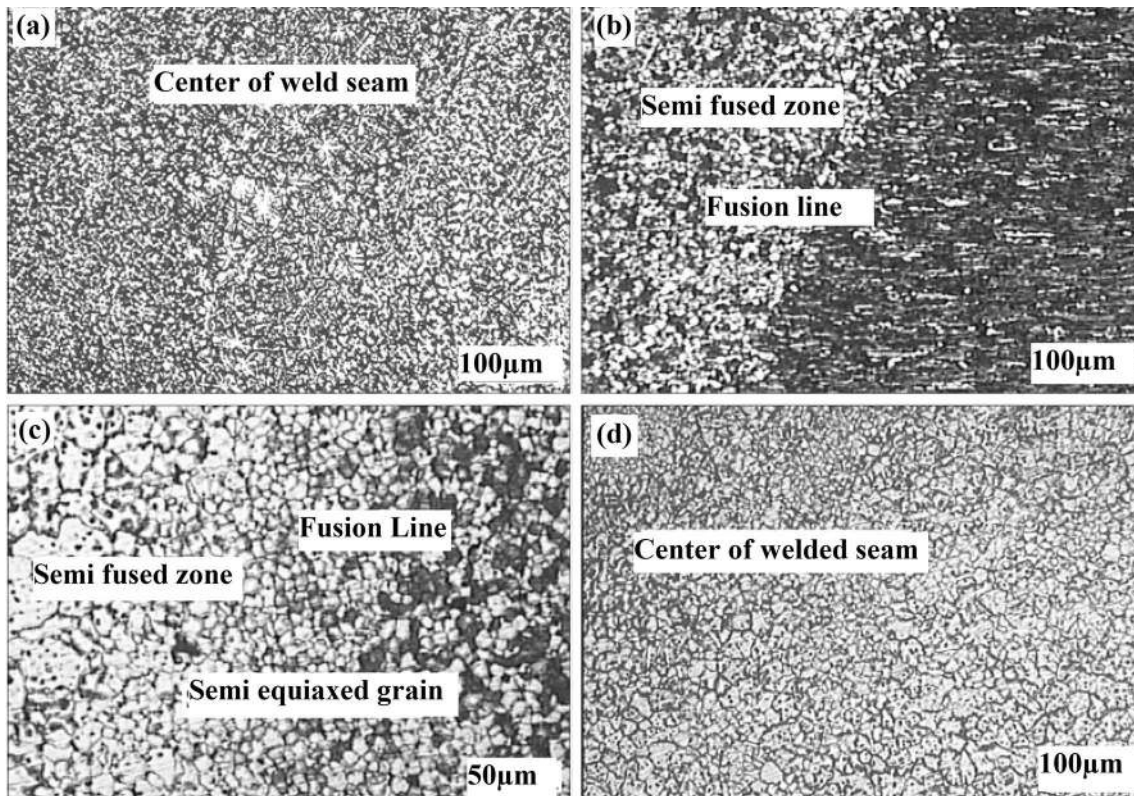


Fig. 8 Optical micrograph of TIG welded joint **a–c** hot rolled plate, **d** cold rolled plate [43]

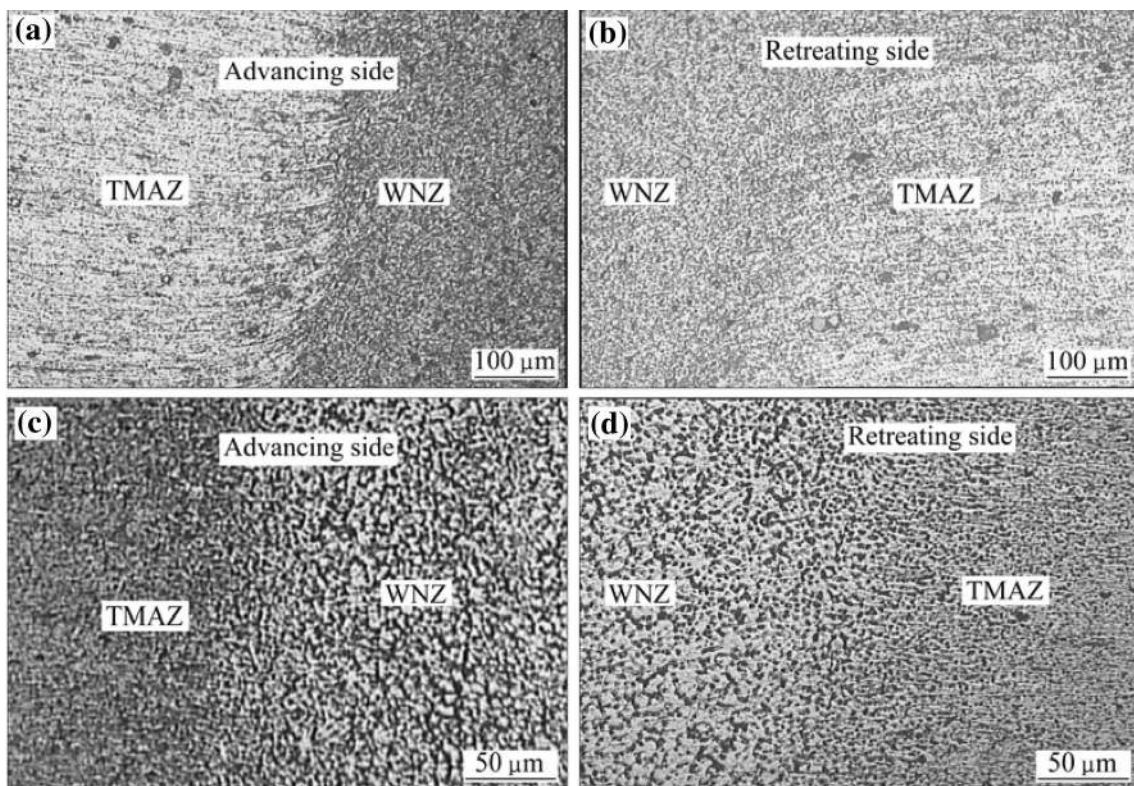


Fig. 9 Optical microstructure of friction stir welded joint, **a** advancing side of hot rolled plate, **b** retreating side of hot rolled plate, **c** advancing side of cold rolled plate, **d** retreating side of cold rolled plate [43]

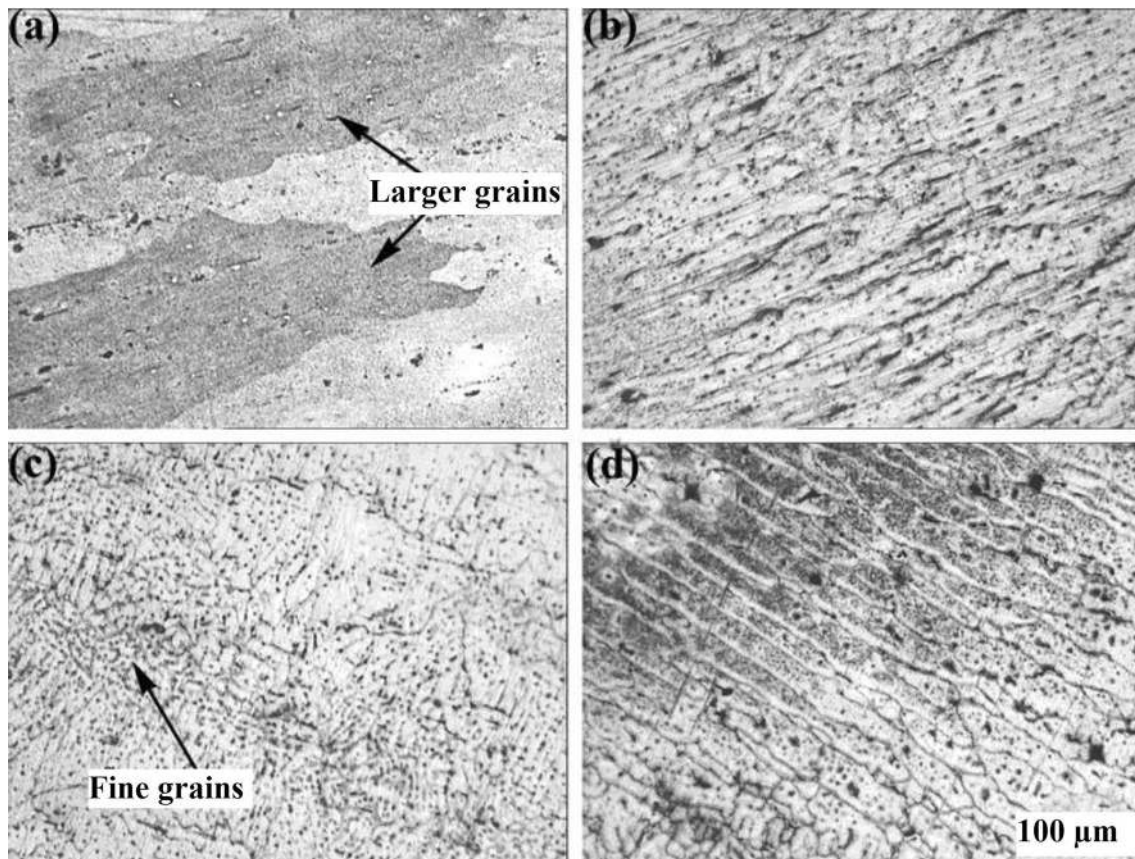


Fig. 10 Microstructure of the TIG welded joint at various zone, **a** parent material, **b** HAZ, **c** fusion zone, **d** partially melted zone [39]

Figure 9 shows the two kinds of welded joint thermo-mechanically zone (TMAZ) and the weld nugget zone (WNZ). The microstructure of weld nugget zone in cold rolled annealed and hot rolled plate were crushed by the strong stirring effect of rotating tool. Because of temperature at weld nugget zone was very high, the dynamic recrystallization takes place small and uniform equiaxed grains emerge at weld nugget zone. The thermo-mechanically zone is weaker heating affected zone than weld nugget zone but stronger than HAZ. The boundary at retreating side is vague and at advancing side is obvious [43]. The relative rate between rotating pin and base metal reached a peak in advancing side and it was the lowest in the retreating side. The stain degree and rate were greater in the advancing side, and the distortion of fibrous microstructure in the advancing side is more severe than that in retreating side [44], which brought the asymmetry of micro-hardness distribution.

Figure 10 shows a microstructure of the TIG weld with the formation of different zone [39]. The grain size of the base metal is completely modified after welding process, and a columnar epitaxial grains can be clearly seen from the HAZ and partly melted zone (PMZ), which are formed

at high temperature adjacent to fusion zone. In this zone, the precipitates which are parent hardened experience a heat treated of over ageing that can cause to phase formation, resulting in deteriorating the mechanical properties of weld [38–40]. It is observed that the microstructure of HAZ and partly melted zone contain coarse and grown epitaxial dendritic grains of α -aluminum and θ -phase [45]. The grown dendritic grains are caused due to the cooling and solidification rate of the weld pool and presence of Mg and other element in the eutectic phase. The presence of insufficient amount of Mg in weld metal resulted in the formation of weak precipitates and not enough to form intermetallic compounds. The zone of the weldments exhibited the micro crack in the grain boundaries where the precipitates and rich in concentration and wider gap between dendrites led to defect formation.

The new approach of using friction stir welding over the TIG welds resulted in a significant improvements in the weld zone. In TIG welding, there are still the presence of porosities in the weld zone, which resulted in the carefully understanding of various spruces of these contaminants to identify the cause and take the necessary actions to get rid of porosities as shown in Fig. 11 [39]. The defect

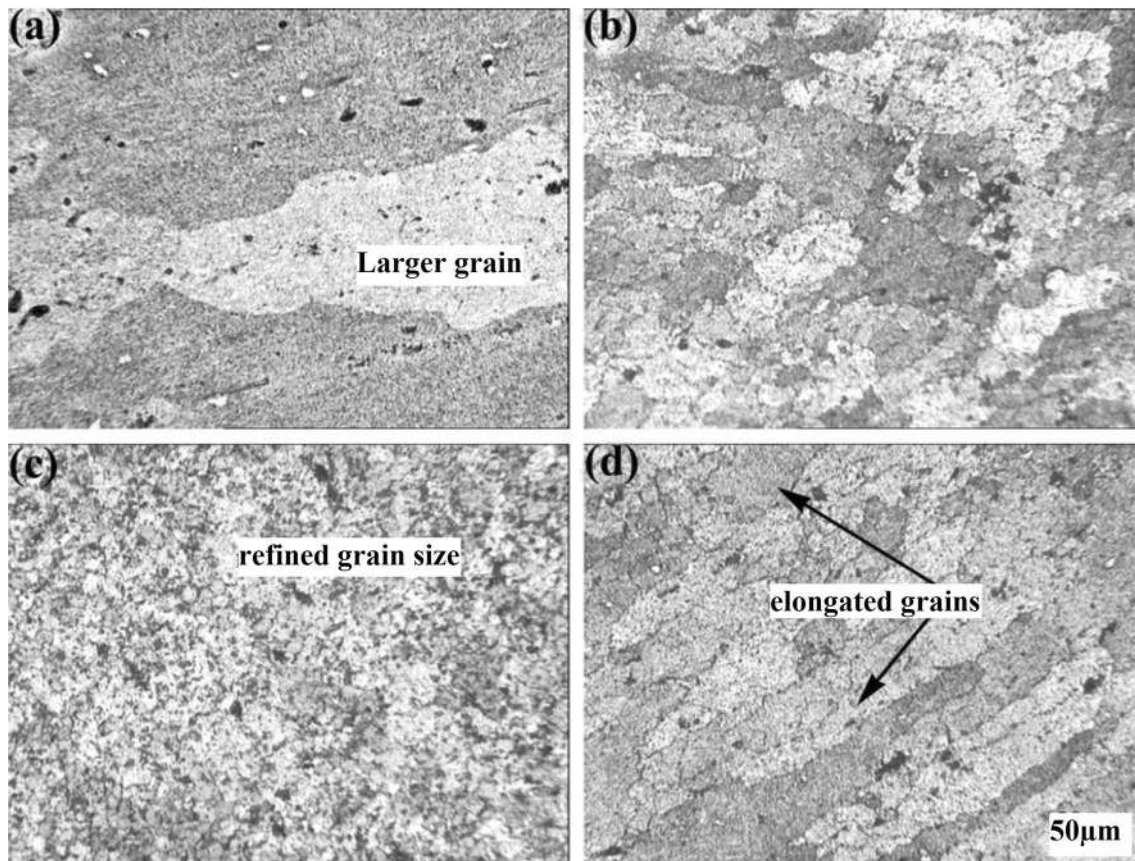


Fig. 11 Microstructure of (TIG + FSP) welds at various zone, **a** base material, **b** HAZ, **c** stir zone, **d** thermo-mechanically affected zone)

free microstructure with the refined grain sizes in the weld zone are depicted in Fig. 11. In this fig, it is found that than coarse and grown dendritic structure are completely modified in the HAZ and TMAZ. It may be due to the breaking of the dendrites and precipitates completely and refined than into a new shape formation as shown the (TIG + FSP) weld microstructure. The grain size of the stir zone is much finer than the TIG fusion zone, there is no evidence of porosity in the weld zone. The small pits also hard to find the TIG + FSP welds and complete defect free weld are achieved. On the other hand, it is worth to mention that the tool motion induces the greater stresses thus resulted in fine grain structure formation, which can allow a partial recovery of the weld metal strength properties and this effect can be seen only on weld nugget [32].

4 Conclusions

A new approach of TIG + FSP process can improve the microstructure and mechanical properties of TIG welded joint. In this study, to avoid coarse grain structure, porosity and micro-crack, friction stir processing is used after Tungsten inert gas welding. FSP is used to destroy the

coarse-grained dendritic structure in the tungsten welded joint and very fine grain structure was observed in stir zone to the effect of intense plastic deformation and temperature during TIG + FSP. The microstructure and mechanical properties of TIG welded joint and TIG + FSP welded joints were studied to understand the behavior of grain structure of both processes. The following conclusions are made during this study.

- The defect and porosity found in TIG weld can completely eliminated by using friction stir processing.
- The friction stir processing over TIG weld completely modified the mechanical and microstructure properties of TIG welded joint.
- The micro-hardness of the TIG + FSP weld is higher than the TIG weld due to fine grain structure in TIG + FSP welds.
- The ultimate tensile strength and elongation of welded joint of (TIG + FSP) are higher than those of TIG and FSW joints, the strength of TIG, FSW and (TIG + FSW) are lower than the parent material.
- The weld nugget zone of friction stir welding and the molten zone of TIG welding are the weakest zone of the welded joints.

Compliance with ethical standards

Conflict of interest On behalf of all authors, the corresponding author states that there is no conflict of interest.

References

1. Thomas WM, Nicholas ED, Needham JC, Murch MG, Templesmith P, Dawes CJ (1991) Friction stir butt welding: PCT/GB92/02203 [P]
2. Mishra RS, Ma ZY (2005) Friction stir welding and processing. *Mater Sci Eng R* 50(1–2):1–78
3. Nandan R, Debroy T, Bhadeshia HKDH (2008) Recent advances in friction-stir welding: process, weldment structure and properties. *Prog Mater Sci* 53(6):980–1023
4. Fonda RW, Knippling KE (2010) Texture development in near- α Ti friction stir welds. *Acta Mater* 58(19):6452–6463
5. Zhou L, Liu HJ, Liu P, Liu QW (2009) The stir zone microstructure and its formation mechanism in Ti–6Al–4V friction stir welds. *Scr Mater* 61(6):596–599
6. Wu LH, Wang D, Xiao BL, Ma ZY (2014) Microstructural evolution of the thermomechanically affected zone in a Ti–6Al–4V friction stir welded joint. *Scr Mater* 78–79:17–20
7. Zhang Y, Sato YS, Kokawa H, Park SHC, Hirano S (2008) Microstructural characteristics and mechanical properties of Ti–6Al–4V friction stir welds. *Mater Sci Eng, A* 485(1–2):448–455
8. Miyazaki M, Nishio K, Katoh M, Mauake S, Kerr W (1990) Quantitative investigation of heat affected zone cracking in aluminum alloy 6061. *Weld Res Suppl* 69(9):362–371
9. Malin V (1995) Study of metallurgical phenomena in the HAZ of 6061-T6 aluminum welded joints. *Weld Res Suppl* 74:305–318
10. Esparza JA, Dvis WC, Trillo AE, Murr LE (2002) Friction stir welding of magnesium alloy AZ31B. *J Mater Sci Lett* 21(12):917–920
11. Meran C (2006) The joint properties of brass plates by friction stir welding. *Mater Des* 27(9):719–726
12. Leitao C, Leal RM, Rodrigues DM, Loureiro A, Vilaca P (2009) Mechanical behaviour of similar and dissimilar AA5182-H111 and AA6016-T4 thin friction stir welds. *Mater Des* 30(1):101–108
13. Satoy S, Yamanoi H, Kokawa H, Furuhashi T (2007) Microstructural evolution of ultrahigh carbon steel during friction stir welding. *Scr Mater* 57(6):557–560
14. Kwon YJ, Shigematsu I, Saito N (2008) Dissimilar friction stir welding between magnesium and aluminum alloys. *Mater Lett* 62(23):3827–3829
15. Christian BF, Murray WM, Mike C (2010) Evolution of microstructure and mechanical properties in naturally aged 7050 and 7075 Al friction stir welds. *Mater Sci Eng, A* 527(9):2233–2240
16. Li Y, Trillo EA, Murr LE (2000) Friction-stir welding of aluminum alloy 2024 to silver. *J Mater Sci Lett* 19(12):1047–1051
17. Peel M, Steuwer A, Preuss M, Withers PJ (2003) Microstructure, mechanical properties and residual stresses as a function of welding speed in aluminium AA5083 friction stir welds. *Acta Mater* 51(16):4791–4801
18. Genevois C, Deschamps A, Denquin A, Doisneau-Cootignies B (2005) Quantitative investigation of precipitation and mechanical behaviour for AA2024 friction stir welds. *Acta Mater* 53(8):2447–2458
19. Rhodes CG, Mahoney MW, Spurling RA, Bampton C (1997) Effect of friction stir welding on microstructure of 7075 aluminum. *Scr Mater* 36(1):69–75
20. Mahoney MW, Rhodes CG, Flintoff JG, Bingel WH, Spurling RA (1998) Properties of friction stir welded 7075-T651 aluminum. *Metall Mater Trans A* 29(7):1955–1964
21. Cavaliere P, Cabibbo M, Panella F, Squillace A (2009) 2198 Al-Li plates joined by friction stir welding: mechanical and microstructural behavior. *Mater Des* 30(9):3622–3631
22. Saini M, Arora N, Pandey C, Mehdi H (2014) Mechanical properties of bimetallic weld joint between SA 516 Grade 65 carbon steel and SS 304 L for steam generator application. *Int J Res Eng Technol* 3(7):39–42
23. Saini M, Arora N, Pandey C, Mehdi H (2014) Preliminary studies on thermal cycling of reactor pressure vessel steel. *Int J Mech Eng* 4(2):51–58
24. Mehdi H, Gaurav S, Kumar T, Sharma P (2017) Mechanical characterization of SA-508Gr3 and SS-304L steel weldments. *Int J Adv Prod Ind Eng* 2(1):41–46
25. Cheepu M, Ashfaq M, Muthupandi V (2017) A new approach for using interlayer and analysis of the friction welding of titanium to stainless steel. *Trans Indian Inst Met* 70:2591–2600. <https://doi.org/10.1007/s12666017-1114-x21>
26. Muralimohan CH, Ashfaq M, Ashiri R, Muthupandi V, Sivaprasad K (2016) Analysis and characterization of the role of Ni interlayer in the friction welding of titanium and 304 austenitic stainless steel. *Metall Mater Trans A* 47:347–359
27. Cheepu MM, Muthupandi V, Loganathan S (2012) Friction welding of titanium to 304 stainless steel with electroplated nickel interlayer. *Mater Sci Forum* 710:620–625
28. Muralimohan CH, Muthupandi V, Sivaprasad K (2014) Properties of friction welding titanium-stainless steel joints with a nickel interlayer. *Proc Mater Sci* 5:1120–1129
29. Cheepu M, Muthupandi V, Che WS (2018) Improving mechanical properties of dissimilar material friction welds. *Appl Mech Mater* 877:157–162. <https://doi.org/10.4028/www.scientific.net/AMM.877.157>
30. Muralimohan CH, Muthupandi V (2013) Friction welding of type 304 stainless steel to CP titanium using nickel interlayer. *Adv Mater Res* 794:351–357
31. Cheepu M, Haribabu S, Ramachandriah T, Srinivas B, Venkateswarulu D, Karna S, Alapati S, Che WS (2018) Fabrication and analysis of accumulative roll bonding process between magnesium and aluminum multi-layers. *Appl Mech Mater* 877:183–189. <https://doi.org/10.4028/www.scientific.net/AMM.877.183>
32. Sutton MA, Yang B, Reynolds AP, Taylor R (2002) Microstructural studies of friction stir welds in 2024-T3 aluminum. *Mater Sci Eng, A* 323:160–166
33. Mishra RS, Ma ZY (2005) Friction stir welding and processing. *J Mater Sci Eng* 50:1–78
34. Mehdi H, Mishra RS (2016) Mechanical properties and microstructure studies in friction stir welding (FSW) joints of dissimilar alloy—a review. *J Achiev Mater Manuf Eng* 77(1):31–40
35. Mehdi H, Mishra RS (2017) Influences of process parameter and microstructural studies in friction stir welding of different alloys: a review. *Int J Adv Prod Ind Eng* 509:55–62
36. Mehdi H, Mishra RS (2017) Mechanical and microstructure characterization of friction stir welding for dissimilar alloy—a review. *Int J Res Eng Innov* 1(5):57–67
37. Mehdi H, Mishra RS (2018) Analysis of material flow and heat transfer in reverse dual rotation friction stir welding: a review. *Int J Steel Struct*. <https://doi.org/10.1007/s13296-018-0131-x>
38. Singh G, Kang AS, Singh K, Singh J (2017) Experimental comparison of friction stir welding process and TIG welding process for 6082-T6 aluminium alloy. In: 5th international conference of materials processing and characterization (ICMPC 2016), proceedings, vol 4, pp 3590–3600
39. Deviredd K, Devuri V, Cheepu M, Kumar BK (2018) Analysis of the influence of friction stir processing on gas tungsten arc welding of 2024 aluminum alloy weld zone. *Int J Mech Prod Eng Res Dev* 8(1):243–252

40. Koteswara Rao SR, Madhusudhan Reddy G, Prasad Rao K (2008) Effects of thermo-mechanical treatments on mechanical properties of AA 2219 gas tungsten arc welds. *J Mater Process Technol* 202:283–289
41. Malarvizhi S, Balasubramanian V (2011) Fatigue crack growth resistance of gas tungsten arc, electron beam and friction stir welded joints of AA2219 aluminium alloy. *Mater Des* 32(3):1205–1214
42. Khan NZ, Khan ZA, Siddiquee AN (2015) Effect of shoulder diameter to pin diameter (D/d) ratio on tensile strength of friction stir welded 6063 aluminium alloy. *Mater Today Proc* 2:1450–1457
43. Zhen-Bo He, Yong-Yi Peng, Zhi-Min Yin, Xue-Feng Lei (2011) Comparison of FSW and TIG welded joints in Al–Mg–Mn–Sc–Zr alloy plates. *Trans Nonferrous Met Soc China* 21:1685–1691
44. Hua Zhang, Lin San-Bao Wu, Lin Feng Ji-Cai (2004) The weld nugget formation of friction stir welded AZ31 magnesium alloy and its affecting factors. *J Aeronaut Mater* 24(6):610
45. Cieslak BA, Zdunek J, Mizera J (2016) Evolution of microstructure and precipitates in 2xxx aluminum alloy after severe plastic deformation. *IOP Conf Ser Mater Sci Eng* 123:1–4
46. Yutaka SS, Kokawa H (2001) Distribution of tensile property and microstructure in friction stir weld of 6063 aluminum. *Metall Mater Trans A* 32(12):3023–3031

Publisher's Note Springer Nature remains neutral with regard to jurisdictional claims in published maps and institutional affiliations.